

# Investigating relationships between cost and CO<sub>2</sub> emissions in reinforced concrete structures using a BIM-based design optimisation approach

S. Eleftheriadis<sup>a,b,e,\*</sup>, P. Duffour<sup>c</sup>, P. Greening<sup>d</sup>, J. James<sup>f</sup>, B. Stephenson<sup>e</sup>, D. Mumovic<sup>a</sup>

<sup>a</sup> Institute for Environmental Design and Engineering, University College London, UK

<sup>b</sup> Department of Computer Science, University College London, UK

<sup>c</sup> Department of Civil, Environmental & Geomatic Engineering, University College London, UK

<sup>d</sup> Faculty of Engineering, Environment and Computing, Coventry University, UK

<sup>e</sup> Price & Myers Consulting Engineers, UK

<sup>f</sup> JAW Sustainability, UK

## ARTICLE INFO

### Article history:

Received 4 July 2017

Revised 18 December 2017

Accepted 28 January 2018

Available online 16 February 2018

### Keywords:

BIM

FEM

Cost

Embodied carbon

RC structures

Optimisation

## ABSTRACT

An integrated design approach for the cost and embodied carbon optimisation of reinforced concrete structures is presented in this paper to inform early design decisions. A BIM-based optimisation approach that utilises Finite Element Modelling (FEM) and a multi-objective genetic algorithm with constructability constraints is established for that purpose. A multilevel engineering analysis model is developed to perform structural layout optimisation, slab and columns sizing optimisation, and slab and columns reinforcement optimisation. The overall approach is validated using real buildings and the relationships between cost and carbon optimum solutions are explored. The study exhibits how cost effective and carbon efficient solutions could be obtained without compromising the feasibility of the optimised designs. Results demonstrate that the structural layout and the slab thickness are amongst the most important design optimisation parameters. Finally, the overall analysis suggests that the building form can influence the relationships between cost and carbon for the different structural components.

© 2018 The Authors. Published by Elsevier B.V.

This is an open access article under the CC BY license. (<http://creativecommons.org/licenses/by/4.0/>)

## 1. Introduction

Structural engineers have traditionally concentrated on the cost efficiency of their designs. The design effectiveness of structural members is critical for exploiting material efficiency and minimising associated construction costs [1]. However, over the last decades, other issues such as the investigation of the structures' environmental performance as well as raising concerns about the overall sustainability of buildings have become more relevant [2–8]. In construction industry one of the most common environmental performance indicators is embodied carbon dioxide [9] and this is the focus of the study. In reinforced concrete buildings, methodological approaches that allow a thorough investigation of the structures cost and carbon performance are still necessary [10]. The reduction of CO<sub>2</sub> emissions in building structures could be achieved not only by considering more sustainable materials but

also by efficiently using structural material through optimisation methods [11]. Recognising trade-offs between carbon and cost efficiencies has been a major challenge for engineering practitioners and researchers for more than a decade. Often it is difficult to take cost-effective decisions without knowing the trade-offs or the relationships between the economic and the environmental performance impacts [12].

Multi-Objective Decision Making (MODM) techniques can provide insights on potential trade-offs between conflicting objectives. MODM techniques are supported by heuristic and metaheuristic algorithms such as Genetic Algorithms, Simulated Annealing, Threshold Acceptance, Ant Colonies, Particle Swarm, Big Bang-Big Crunch, Artificial Neural Network etc. and they have been extensively used in theoretical as well as practical problems in civil and structural engineering [13–22]. These stochastic search methods implement a combination of rules and randomness functions that appear in most natural systems including survival of the fittest, natural selection, memory, visibility, discrete time, swarm behaviour [23–25]. In principle, these techniques tend to produce a good approximation of the optimum solution with reasonable computational costs

\* Corresponding author at: University College London, Institute for Environmental Design and Engineering, 14 Upper Woburn Place, London WC1H 0NN, UK.  
E-mail address: [efstathios.elftheriadis.13@ucl.ac.uk](mailto:efstathios.elftheriadis.13@ucl.ac.uk) (S. Eleftheriadis).

[26,27]. A detailed survey of metaheuristics optimisation can be found in Boussaid et al. [28].

Several studies have explored optimal design solutions using MODM techniques considering both economic and environmental aspects reinforced concrete beams [6,29,30], reinforced concrete frames [31,11,32], reinforced concrete columns [33,34]. Previous studies have investigated the relationship between carbon and cost optimum designs on different structural systems. In Camp and Assadollahi [2], carbon optimum solutions are only 2.5% more expensive than the cost optimum designs. In Camp and Huq's [31] and Paya-Zaforteza et al's [11] study of RC frames carbon optimum solutions cost 2% and 2.8% respectively more than the low-cost options. Yepes et al. [9] have reported an increase of 1.3% in cost of the carbon optimum solution. Finally, Martinez-Martin et al [5] have found an almost linear relation between cost and carbon objectives in their optimisation analysis of reinforced concrete bridge piers.

From the previous literature review it is observed that most of the optimisation studies have focused on isolated components of the structure. In flat slab structural systems which are widely used by practitioners, understanding the relationships between cost and carbon optimum solutions for the entire structure as well as for the different structural components such as slabs, columns, structural grids can provide useful insights for early stage sustainable design decisions. In the past, most of the studies on flat slab optimisation have focused on cost optimisation [35] or cost and layout optimisation [36] using the Equivalent Frame Method (EFM). Only recently Aldwaik and Adeli [37] have suggested a Finite Element Model (FEM)-based cost optimisation of flat slabs without looking at the carbon implications or layout optimisation. Foraboschi et al. [38] have studied the impacts of floor selection on the total embodied energy in tall building structures with more than 20 storeys. The implementation of lightweight floors does not necessarily mean less embodied emissions but depending on the architectural requirements the overall number of columns could significantly reduce the material used in floors and beams. Fernandez-Ceniceros et al. [39] have introduced a decision support model based on three decision trees for the design of one-way floor slabs for a case study in Spain. To find environmentally friendly and cost-effective solutions their model considers both embodied carbon and total initial slab costs. For floor spans of 6–7 m they observed that up to 20% reductions in CO<sub>2</sub> could be achieved with a corresponding cost increase of less than 6%.

Despite the various algorithmic approaches for the optimisation of building structures that have been developed in the past, the practical implementation of such methods is very limited in real design situations. The lack of integration with collaborative design workflows is an important limitation of the current methods. However, the development of Building Information Modelling (BIM) offer opportunities that could effectively consolidate structural MODM in buildings sustainability domain for early decision-making whilst BIM-integrated optimisation procedures could offer new ways to increase the adoption levels of structural optimisation techniques in practice [40]. In fact, the capabilities of BIM technologies have not been appropriately utilised in the optimisation of reinforced concrete structures even though BIM-enabled optimisation methods have been introduced for other structural material such as steel in the past [41].

Previous optimisation efforts in RC building structures focused on either columns, or beams or frames or floor optimisation independently. However, the singular analysis approach could limit the understanding of the whole structural system's behaviour. The use of BIM by practitioners could act as a driver for novel optimisation paradigms that deliver more integrated structural optimisation approaches offering a better understanding of the interactions

between the structural components and the rest of the building systems.

To address these limitations, the paper examines a BIM-integrated optimisation approach to simultaneously assess the cost and carbon performance of RC building structures with flat slabs and columns which is a very common building typology. A FEM structural optimisation engine using BIM and a heuristic multi-objective optimisation algorithm – Nondominated Sorting Genetic Algorithm II (NSGA-II) was developed for that purpose. The embodied carbon and cost analyses focus primarily on the material production stages. To achieve a comprehensive optimisation for the entire structure a multilevel computational model is developed that involves: (1) structural grid layout, (2) slab and columns sizing, and (3) slab and columns reinforcement. The paper is organised as follows. Section 2 summarises the general research approach including the optimisation algorithm and the BIM integration. The multilevel optimisation model for the analysis of the structure is also specified in Section 2. In Section 3 the implementation of the optimisation model in practical examples and the cost and carbon analysis are presented and discussed. The paper concludes in Section 4.

## 2. Research methodology

### 2.1. Optimisation workflow

The flow diagram of the proposed optimisation is shown in Fig. 1. BIM is the core of the proposed integrated architecture offering: (1) the source of input data for the optimisation analysis, (2) the platform for the visualisation of optimisation analysis outputs. The implementation of BIM technologies not only improves the way optimisation-related data are mined and queried but ultimately it could also speed up the adoption of such analyses in practical circumstances. The optimisation approach starts from an early stage BIM model, which involves basic geometric information about the building. The notion is that the development of the structural solution will be developed collectively by the structural engineers using the proposed optimisation and the rest of the design team who will assess the optimised designs directly in BIM. The BIM model is used to create the geometric boundaries of the structural floors which are computed in FEM. Data relevant to the structural analysis such as load cases, material properties and code limits are also incorporated at this stage.

The input parameters for the optimisation algorithm describe the boundaries of the solution space. The optimisation parameters are identified by structural engineers based on project specific information using a custom Graphic User Interface (GUI) which was developed for that purpose. This interactive approach effectively restricts the solution space in the areas where the engineers find more suitable for the project based on their previous experience. Design and detailing data ranges for the seven optimisation input parameters (genes) are provided by the GUI and include (1) Slab thickness, (2) Column width, (3) Column height, (4) Number and length of column grid in X direction, (5) Number and length of column grid in Y direction, (6) Number of bars in columns' width, (7) Number of bars in columns' height. At every iteration, the algorithm assigns a random value to every input parameter from a predefined list to individuals in the population, which represent a structural design configuration.

The population consists of individuals that are evaluated based on specific cost and embodied carbon objective functions. Underperforming individuals are removed from the population as it evolves. Well-performing individuals receive higher ranking and climb the population list and ensure their genes are transferred in future generations. Crossover and mutation operators are used in the NSGA-II to evolve the population. The structural system that

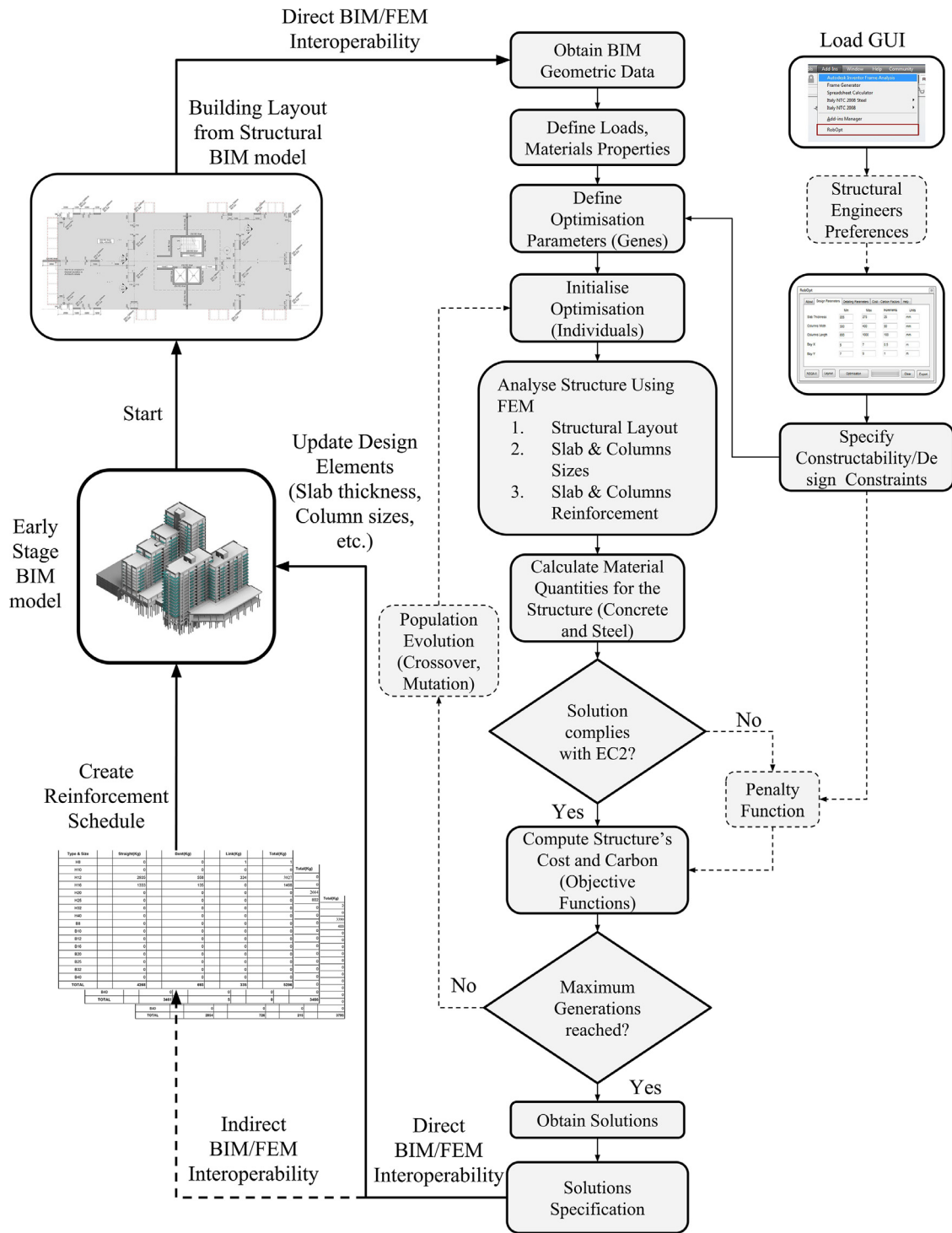


Fig. 1. Flow diagram of the integrated optimisation approach and its main components.

is created based on the input parameters is then evaluated using FEM and the material listings of the structure are obtained for concrete, reinforcing steel and formworks. The classification of material quantities is organised based on the different BIM object families. In this study the structural functional unit includes floors and columns and thus they have a dedicated material quantity type.

An essential step in the process is the verification with the national or international structural codes. In this study the Eurocode (EC2) has been used to validate the structural performance. The prescribed loads in the structure are also defined through the GUI

by the structural engineers. If the verification of the structure does not comply with EC2 limit states (e.g. deflections) or other constructability restrictions which are identified by the structural engineers using the GUI the solution receives a penalty function. The penalisation step ensures the algorithm eliminates designs from the population that are not complying with the structural or constructability constraints. Models from [42] were implemented to ensure the effective tuning and implementation of the penalty function in the optimisation procedure which is a minimisation problem with  $m$  constraints. Using the material listings and the

penalty functions, both the cost and carbon objective functions are then calculated. Conversion factors were incorporated in the objective functions to calculate the final cost and embodied carbon of the structure and its components. Cost and carbon data from literature were used for the conversion factors (Refer to Section 3.2 for detailed cost and carbon factors). The cost and carbon performance of each individual is then used to update the population information on each generation until the maximum number of allowable generations set by the user is reached. The optimisation process ends with the generation of the non-dominated structural design solutions when none of the objective functions can be further improved without compromising the other objective function. After the optimisation results are evaluated by the structural engineers the design and detailing components are transferred back into the structural BIM model. A body of work examining the consequential effects of optimised structural designs in the entire building lifecycle performance within BIM is also planned. The BIM-based optimisation will contribute towards these studies as comprehensive lifecycle analysis could be effectively delivered using the results obtained from this integrated optimisation module.

## 2.2. BIM integration

The interoperability between FEM and BIM is an important parameter for the computation and delivery of the proposed optimisation process. With regards to BIM architecture, *Autodesk Revit 2016* was used and *Autodesk Robot (RSA) 2016* was selected as the FEM engine, due to their wide applications in industrial and academic projects. There is a direct interoperability function between BIM and FEM which allows design elements, geometric layouts and material properties to be transferred from BIM to FEM and vice versa. The default data exchange capabilities between *RSA* and *Revit* are further amplified by accessing the API of *Revit* and *RSA* for customised data processing. This indirect BIM/FEM interoperability was implemented in more complex data structures which are generated by the FEM computations. In this research, C# were implemented to access the .NET framework of *RSA* and *Revit* APIs using Visual Studio 2013. The API provides control over the following attributes of the structural analysis [43]: geometry generation and manipulations, model structural analysis, structural sizing and property assignment, analysis runs (linear, nonlinear) and result evaluation (stresses, deflections, member forces) and code verification.

Two BIM-enabled functionalities are implemented in the proposed optimisation: (1) Data required for the optimisation of the structure have been obtained from BIM (Downstream), (2) Data obtained from the cost and carbon optimisation of the structure are returned in BIM (Upstream). Downstream the topology of the floor is directly imported from BIM and transferred into the structural analysis component (FEM) where all coordinates, dimensions and material properties are recognised and translated into structural components. At that stage the optimisation algorithm begins its operations. The optimisation approach takes place as shown in Fig. 1. At the end of the optimisation the obtained structural designs are evaluated by the structural engineers. Selected alternatives are returned into BIM for further analysis at building level from the design team. Upstream the information transferred back in the BIM model involves two main components: (1) Geometric or design elements of the structure such as slab thickness, columns sizes and grids using the direct interoperability functions, (2) Detailed reinforcement schedules and quantities using the indirect interoperability functions based on .csv data exchange. The indirect interoperability process was made possible through the detailed implementation of the API functionalities of *RSA* and *Revit*. Once the optimisation computations are completed, reinforcement data relevant to each design configuration of the Pareto front are

temporarily stored in csv files using *RSA*'s API. The bar diameters sizes ( $\emptyset 10$ ,  $\emptyset 12$ ,  $\emptyset 16$ ,  $\emptyset 20$ , etc.) and their frequency of occurrence in the different building elements (total number for each bar size), are organised using the relevant BIM element fields and levels. For each of the reinforcement options, the mass summaries (in kg) are used directly as calculated from the optimisation analysis. The data from the output csv file are then read using the *Revit* API to modify the material schedules for the reinforcement quantities in the BIM model. At this stage of the research the reinforcement data are used only as schedules and not as a new design element (reinforcement topology) in the BIM model.

## 2.3. Optimisation algorithm formulation

A modified NSGA-II algorithm developed in C# is implemented herein to analyse both cost and carbon objective functions embedding the FEM engine. The aim of the multi-objective solver is to find the relationships between the cost and carbon objective functions to inform early design decisions associated with the RC structure.

### 2.3.1. NSGA-II algorithm

The set of trade-off solutions is known as the set of non-dominated Pareto optimal solutions. NSGA-II was introduced by Deb et al [44] and is considered as one of the most powerful and widely used multi-objective optimisation methods [45] that effectively approximates the Pareto front in computationally intense problems such as structural optimisation problems that involve FEM analyses. For the purposes of this study the NSGA-II algorithm was modified in C# using the API of *RSA* to accept FEM data and it is based on two objective functions that involve embodied carbon emissions and cost of the structure.

### 2.3.2. Objective functions

In the carbon optimisation module, the embodied carbon of the structural system is minimised: in the function  $f_{ec}: E \rightarrow \mathbb{R}$  from some set  $E$ , the algorithm is searching for the element  $x_0$  in  $E$  such that  $f_{ec}(x_0) \leq f_{ec}(x)$  for all  $x$  in  $E$ . The objective function is constructed to include the embodied carbon of the structural elements.

$$f_{ec}(x) = \sum_{i=0}^n q_i e_i \quad (1)$$

where  $q_i$  are the quantities obtained from the FEM structural analysis and  $e_i$  is the carbon factors for the concrete, reinforcement and formwork components. The carbon factors are based on CEN/TC350 framework. CEN/TC350 is responsible for the development of standardised methods for the assessment of the Life Cycle Assessment (LCA) aspects of new and existing construction works (buildings and civil engineering works), including horizontal core rules for the development of Environmental Product Declaration (EPD). EPD data were used to obtain regional verified and registered data about common structural materials [46]. Because most of the lifecycle carbon emissions of building structures are associated with the initial embodied carbon [46], in this optimisation study data from the material and product stage (A1–A3) were used in the carbon factors of the concrete, reinforcement and formworks to simplify the calculations. Stages A4–5, B, C and the benefits and loads beyond the system boundary (Stage D) could be integrated on a case-by-case basis and are not included in the scope of this study considering the well recorded limitations of embodied carbon [47] and lifecycle [48] assessments. The final carbon results are calculated in  $\text{kgCO}_2\text{e/m}^2$  using the gross floor area of the building. Even though priority was given to EPD data, evaluating the uncertainty of the obtained data was necessary to ensure the robustness of the performed analysis. According to Webster et al. [49], the



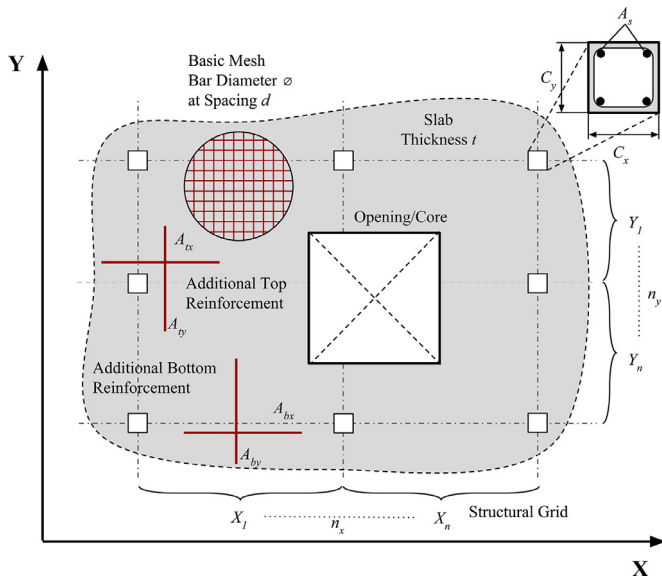


Fig. 2. Demonstration of structural optimisation levels.

uncertainty in the embodied carbon factors can be caused by the quality (consistency, geography, etc.) or the variability (production, material specification, etc.) of the obtained data. Herein, Gregory et al.'s [50] method for robust comparative LCA was considered for the evaluation of the embodied carbon factors uncertainties. After reviewing databases such as ICE, GaBi, EcoInvent and Athena, the following variations were identified for the main structural materials: (1) Concrete 0.08 to 0.22 kgCO<sub>2</sub>e/kg, (2) Rebar 0.59 to 1.70 kgCO<sub>2</sub>e/kg [46].

In the cost optimisation module, the construction cost of the structural system is minimised: in the function  $f_c: E \rightarrow \mathbb{R}$  from some set  $E$  the algorithm is searching for the element  $x_0$  in  $E$  such that  $f_c(x_0) \leq f_c(x)$  for all  $x$  in  $E$ . The objective function is defined to include the construction costs which incorporate material and labour costs of the structural elements:

$$f_c(x) = \sum_{i=0}^n q_i c_i \quad (2)$$

where  $q_i$  are the quantities obtained from the FEM structural analysis and  $c_i$  is the cost factors for concrete, reinforcement and formwork. The construction cost is calculated by multiplying the cost factors for the different material with their corresponding quantities. All cost data are collected from Spon's Architects' and Builders' Price Book 2017 [51]. As the cost factors have different units, appropriate conversion factors were used in the algorithm. For the calculation of the total costs the individual components are added together and divided by the total floor area (€/m<sup>2</sup>).

#### 2.4. Multilevel optimisation model

In this study, the optimisation approach occurs in three engineering analysis levels that are associated with the structural grid topology, sizes of columns and slab, and reinforcement rates for columns and slab. The integration of these three levels into a single optimisation approach is significant as it offers a comprehensive design analysis procedure for early design development. In addition, it provides an overview of the impacts from the different structural components in both cost and embodied carbon.

##### 2.4.1. Optimisation levels

Fig. 2 shows a representation of a general structural system with the corresponding design variables used in the optimisation

procedure. These involve  $t$  = slab thickness,  $A_s$  = columns reinforcement,  $\{A_{tx}, A_{ty}\}$  = Additional top reinforcement in the slab,  $\{A_{bx}, A_{by}\}$  = additional bottom reinforcement in the slab,  $\{X_i, Y_j\}$  = bay lengths,  $\{C_x, C_y\}$  = columns sizes under investigation.

Structural cores were included in the algorithm for lateral stability and vertical support mainly but they were not optimised. The optimisation algorithms developed in this research use these highlighted parameters as inputs to define the design solution space. Discrete variable ranges have been used throughout to represent the optimisation input parameters. To increase the feasibility of the solution space the selection of optimisation parameters utilises an expert input approach which involves the preferences from engineering practitioners based on project specific requirements. For example, the slab thickness could typically take any value between 200 mm to 300 mm for common buildings but in reality structural engineers will only specify from a limited number of slab options (2 or 3) depending of the building type and conditions. Similar filtering procedures apply in the rest of the design optimisation parameters. This is a main motivation behind the proposed computational framework which synthesises design inputs by structural engineers to improve the quality of the optimisation search. This is beneficial for three reasons: (1) the design solutions are actual design configurations the structural engineers could test and propose in practice for validation or comparison purposes, (2) the design search can be more focused and efficient based on structural engineers' preferences without the need to investigate large design spaces, (3) the project engineers are actively involved in the optimisation procedure as they can directly influence its outputs. Several customised algorithms have been developed to perform these computations, which are elaborated in the subsequent sections.

##### 2.4.2. Structural layout

The structural layout ( $X_i, Y_j$ ) is a critical design parameter that is normally defined early in the process. The complexity or rationalisation of the column grid is greatly influenced by the building use. Early decisions on the grid have major impacts on the detailed design of the slab and columns. A computational module was developed to enable automatic generation and optimisation of the structural column grids. The algorithm reads the relevant floor boundary lengths obtained from the BIM model and uses them to compute all possible configurations of the structural grid on x- and y- directions within a finite discrete set. This approach can be implemented in any floor layout geometry from the BIM model which increases the application potential of the model. The algorithm uses combination and permutation components to find the necessary column configurations. To resemble realistic conditions, structural engineers assign possible span lengths that they want to investigate. Common spans for RC flat slab systems vary between 5 m and 9 m. The proposed algorithm any length increments the structural engineers deem necessary. Once the allowable span lengths are assigned by the user, the recursive algorithm computes all possible number of bays and bay length combinations that match the boundaries of the slab. The resulting combination lists are used as input data in the permutation algorithm which computes all possible configurations based on the generated span lengths whilst removing any duplicate data configurations. For the example in Fig. 3 assuming  $x_{total} = 35$  m more than 2000 structural grid configurations are generated from the algorithm ranging from 4-bay options {9 m, 9 m, 9 m, 8 m} to 5-bay {5 m, 5.5 m, 7 m, 8.5 m, 9 m}. The results from the algorithm are stored in a temporary two-dimensional list and accessed by the algorithm when searching for the optimum grid configuration.

##### 2.4.3. Sizing

The design variables for the slab depth ( $t$ ) dimensions are discrete variables based on constructability limitations which are de-

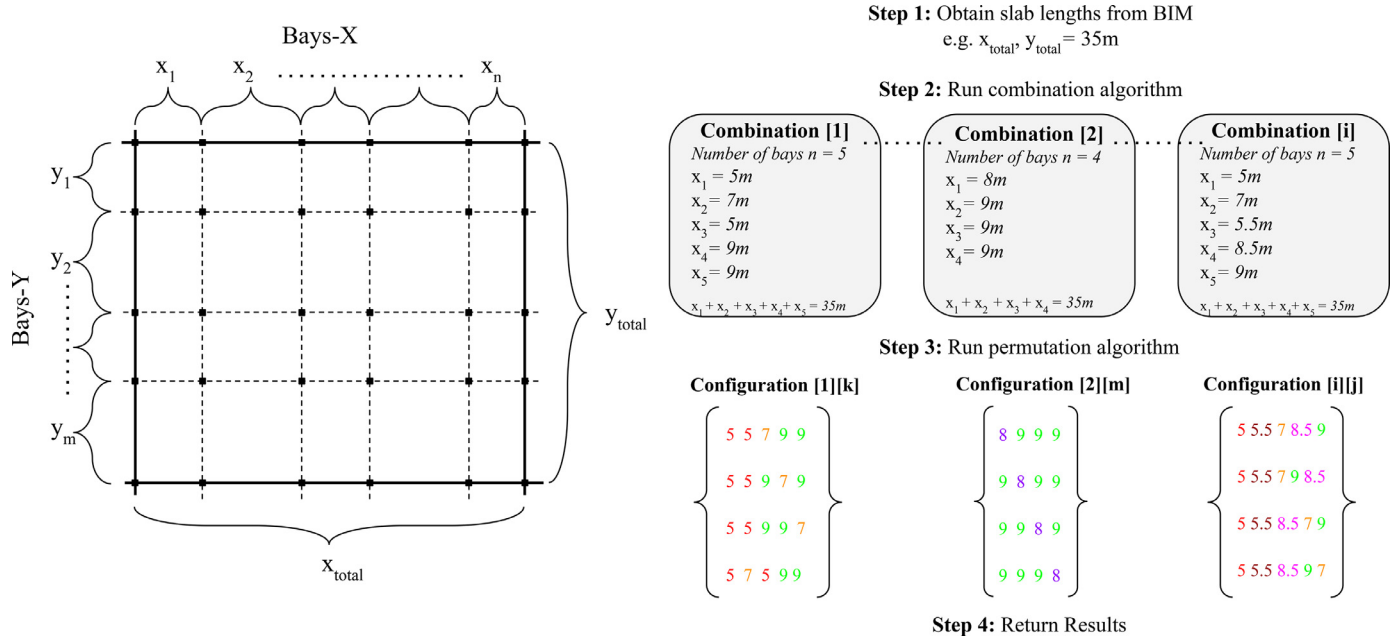


Fig. 3. Representation of the structural layout computations.

fined by the structural engineers in the GUI. The data are encoded into input arrays and the algorithm randomly selects a component of the list during each FEM iteration. Furthermore, discrete variables are used for the sizing optimisation of the RC columns ( $C_x$ ,  $C_y$ ). A penalty function was used to ensure the columns width-to-depth ratios are constrained to 4:1. Other sizing restrictions could be implemented in the algorithm depending on project-specific conditions. For example, to ensure that the columns are effectively integrated within the internal walls their width could also be limited to the wall thickness which is provided by the architects Overall, all variables used in the sizing optimisation module could be adjusted to user specified limits.

2.4.4. Detailing

The section describes the way the structural reinforcement calculations are performed in the optimisation process. At the detailing level of the optimisation the reinforcement quantities in the slab and columns are computed. The slab reinforcement consists of the basic mesh that is applied everywhere and additional top ( $A_{tx}$ ,  $A_{ty}$ ) and bottom ( $A_{bx}$ ,  $A_{by}$ ) reinforcement bars only in the zones that are necessary. For the columns bending reinforcement ( $A_s$ ) is calculated. All designs are compliant with the Eurocode’s requirements. This module does not only provide general reinforcement rates but establishes detailed reinforcement schedules and layouts which can significantly reduce analysis time in real projects. This set of analysis consists of several algorithmic components.

- Slab reinforcement computations

For the computation of slab reinforcement, a novel design algorithm is developed which not only calculates reinforcement rates but also provides detailed reinforcement schedules and layouts. The punching shear reinforcement has not been included in this analysis as it is usually estimated at a later stage of the design. The FEM analysis in RSA identifies the required reinforcement areas ( $mm^2/m$ ) in the slab. Coons’ method [52] is used to generate the finite mesh in the slab and the Wood and Armer method [53,54] is used in the calculation of the moment for the required reinforcement in the slab. The algorithm reads the data from all the Finite Element (FE) mesh points in the model (4 edge nodes and 1 central node) and calculates the minimum and maximum values of re-

quired reinforcement as shown in Fig. 4. The minimum values are used for the estimation of the basic reinforcement mesh, whilst the difference between maximum and the minimum values are used for the calculation of the additional reinforcement.

Once all individual (FE) mesh components are obtained, the algorithm identifies the overall minimum required reinforcement values that are larger than zero and assigns the basic reinforcement mesh from a list of predefined reinforcement rates. Constructability constraints on the available bar diameters and spacing are incorporated. The bar diameters are limited to the most common diameters that engineers use in practice whilst their spacing also follows practical increments. The total quantities (in kg) of basic reinforcement is then calculated by multiplying the reinforcement rate with the area of the slab panel.

One of the main aspects of this algorithm is the implementation of a retention function. The bar spacing specified in the basic reinforcement mesh is stored in the system and can be accessed during the computation of the additional reinforcement. Once the basic mesh reinforcement is calculated, the variances between the assigned basic reinforcement area and the maximum mesh/node values of the required reinforcement are computed to estimate the area of the additional bars. Each component of the mesh carries a digital identity which is used in this component to identify the zones in need of additional reinforcement.

A zoning algorithm is implemented to resemble practical ways of arranging the additional reinforcement. For the additional bars the algorithm searches again the available reinforcement database for values that match the spacing of the basic mesh which was stored in the previous algorithm. For example, if the basic mesh is  $\phi 12$  at 250 mm centres the additional reinforcement would also be spaced at 250 mm to enhance constructability. Another component of this algorithm involves the direction of reinforcement (X or Y) which is used for horizontal and vertical zoning. The algorithm reads the data from the individual zones and finds the maximum value which thereafter is applied to the adjacent zones that are not zero. This approach offers practical zoning of the additional reinforcement on the slab and can be used in both X and Y directions for top and bottom reinforcement calculations. The total quantity of reinforcement is the sum of the basic mesh weight and the weight of the additional reinforcement in kilograms or tonnes.

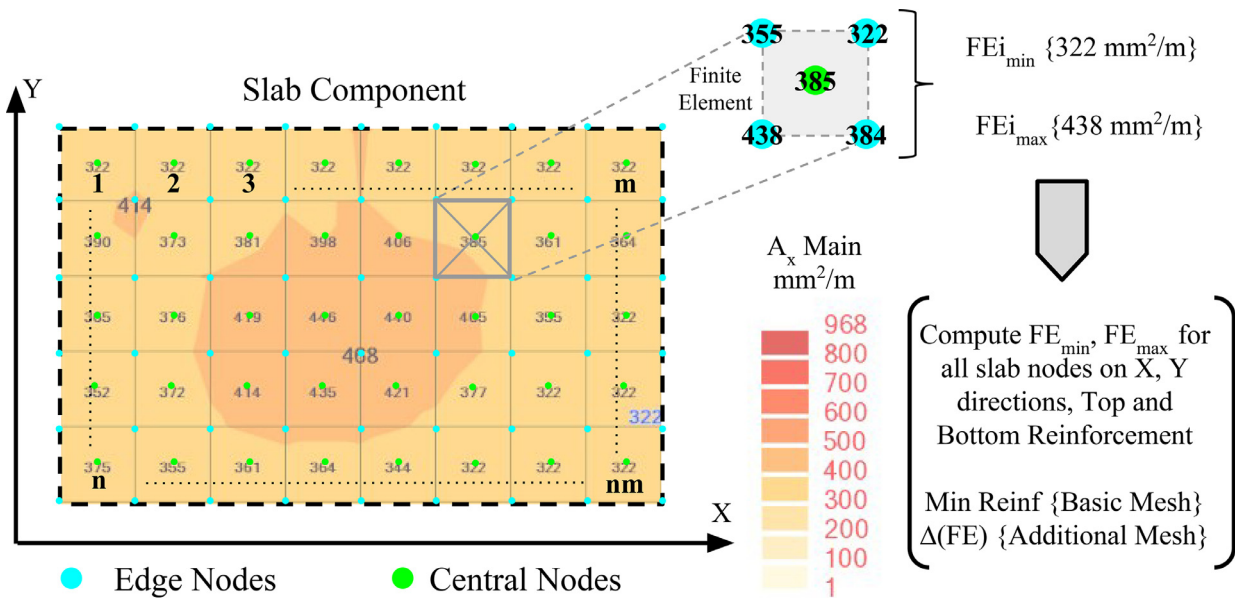


Fig. 4. FEM Initialisation process of required reinforcement computations.

#### - Columns reinforcement computations

For the calculation of the bending reinforcement in the columns another algorithmic component is implemented. This component uses forces (reaction loads), geometric (column cross section, storey height) and material data from the structural model in RSA. It then transfers that data into a custom Excel spreadsheet where the compliance checks take place and the suitability of each section is verified. When all checks are verified, the approved reinforcement is obtained from the calculation spreadsheet and the material quantities for the columns are updated in the objective functions of the optimisation.

### 3. Practical examples

Actual building scenarios were used to verify the aforementioned optimisation approach. The buildings were selected based on their aspect ratio in order to investigate the influence of the building form in the optimisation results and particularly in the relationships between the cost and carbon performance of the different structural components. Two representative building scenarios were analysed herein. Case Study 1 ( $CS_1$ ) has an aspect ratio of 2:1 in plan, whereas Case Study 2 ( $CS_2$ ) has an aspect ratio of 1:1. The details of the case studies are provided in the subsequent sections and the typical building layouts are shown in Fig. 5.

In both instances, the structural core was in the centre of the building which is representative for multistorey residential buildings as it provides the space for vertical circulation. Nonetheless, other core layout configurations could also be analysed without significant alterations in the computational components of the optimisation model. The numerical examples include two main parts. Firstly, the conventional designs as proposed by the project engineers are analysed by reviewing their cost and embodied carbon performance. The second part presents an analysis of the optimised designs developed by the cost and carbon optimisation approach. The intention of this analysis is not only to create a direct comparison between the conventional and the optimised designs but to use the optimised solutions as cost and carbon benchmarks for the given set of design parameters. Even though the numerical assessment of the results is relevant to the case studies, the proposed

optimisation method can easily be generalised as it can be applied in any BIM structural model.

#### 3.1. Buildings description

##### 3.1.1. Case study 1

$CS_1$  is part of a larger residential apartment block in London, UK ranging between 9 and 17 storeys. The proposed superstructure is a reinforced concrete frame with stability provided by RC shear walls. The cores have been designed to support the full lateral load with no contribution from the blade columns. The structural floor is a flat slab with 250 mm in thickness. The load cases in this building include superimposed dead loads (SDL), live loads (IL) and dead load. For the residential areas, it is assumed  $SDL = 1.6 \text{ kN/m}^2$  and  $IL = 1.5 \text{ kN/m}^2$  uniformly distributed on the whole floor. In addition, the cladding load on the edges of the slab is  $SDL = 1.5 \text{ kN/m}$  and for the balconies it is assumed  $SDL = 3.7 \text{ kN/m}$  and  $IL = 5 \text{ kN/m}$ .

##### 3.1.2. Case study 2

$CS_2$  is a 10-storey residential tower in London, UK. The column grid proposed by the project engineer is 7.5 m generally to match the architectural grid. The cladding of the building is masonry, with lightweight metal studwork to the inner skin of the cavity walls. The structural floor is a flat slab with 275 mm in thickness. The structural loads are  $2.45 \text{ kN/m}^2$  and  $2.5 \text{ kN/m}^2$  for imposed dead and live loads respectively. The following load combination cases according to the Eurocode were considered in the analysis of both cases studies from the engineers:  $ULS = 1.35G + 1.5Q$  and  $SLS = G + Q$ ,  $SLS = G + 0.3Q$ . All vertical elements and slabs in both buildings are C32/40 with columns to be C50/60.

#### 3.2. Conventional design results

##### 3.2.1. Assumptions

The cost and carbon of the slab and the columns are estimated utilising the cost and carbon functions presented in Section 2.3.2 and the material schedules obtained from BIM data models. Detailed reinforcement layouts were used to calculate accurate tonnage of steel in the slabs and columns. The material specifications from the actual projects were advised where possible

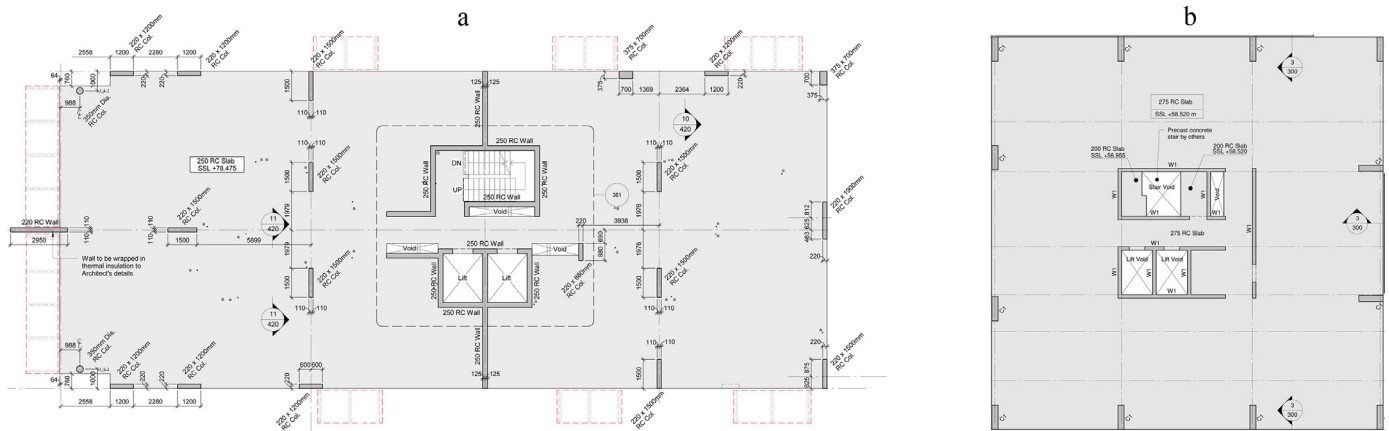


Fig. 5. (a) Case Study 1 (b) Case Study 2.

to define the relevant cost and carbon factors. The carbon factors (Stages A1–A3) for the concrete are  $C_{40} = 130 \text{ kgCO}_2\text{e/t}$ ,  $C_{50} = 170 \text{ kgCO}_2\text{e/t}$  [55] and the steel reinforcement  $1270 \text{ kgCO}_2\text{e/t}$  [55]. It can be observed that the EPD data fall within the available ranges recognised from the literature in Section 2.3.2. Virgin steel rebar was specified in the actual projects and thus the same assumption was made in the analysis. In addition, the carbon factor for the columns formwork is assumed  $8.9 \text{ kgCO}_2\text{e/m}^2$  [31] and for the slabs  $3.14 \text{ kgCO}_2\text{e/m}^2$  [56]. If project specific carbon data are not available then assumptions about the origin and the uncertainties of material databases would be necessary. A comprehensive review on this topic can be found in [47].

### 3.2.2. Design analysis

In  $CS_1$  the reinforcement rate in the slab is approximately  $112 \text{ kg/m}^3$ . The slab reinforcement consists of  $\phi 12$  bars (13.3 tonnes) and  $\phi 16$  bars (3.2 tonnes) which are common bar diameters used in practice. With regards to the structural elements dimensions, the slab thickness is fixed to 250 mm and the lengths of the columns (20 in total) vary from 700 mm to 1500 mm. The thickness of the columns is governed by the thickness of the walls which is limited to 220 mm in most cases. Reinforcement bars of 16 mm and 20 mm in diameter were used in this analysis for the typical columns case. In  $CS_2$ , the slab reinforcement rate is  $157 \text{ kg/m}^3$  and the bars are also  $\phi 12$  (4.5 tonnes) and  $\phi 16$  (14.6 tonnes). The upper level slabs are 275 mm thick and the dimensions of the twelve columns are  $200 \text{ mm} \times 800 \text{ mm}$ . The reinforcement in the twelve columns consists of 16 mm bars. In both buildings, the slab deflections were limited to 30 mm.

### 3.2.3. Cost and carbon assessment

The carbon and cost distribution in the entire structure for both case studies are shown in Fig. 6(a) and (b) respectively. The results for the  $CS_1$  indicate that the floor is responsible for 83% of the total costs of the structure when only 17% can be attributed to the costs of the columns. The carbon analysis shows that 87% of the total embodied carbon in the structure is due to the slab impacts whereas the columns are responsible for only 13% of the total carbon. On the other hand, in  $CS_2$  the floor is responsible for the 93% of the total costs and the remaining 7% is attributed to the columns. Similarly, the slabs comprise 95% of the total carbon when the columns are responsible for only 5%. In both instances the results are not surprising as the slab covers a large proportion of the structures volume which thus affects the final cost and carbon rates. However, it was observed that there is a 10% difference in the cost and carbon distribution between the slabs and the columns of  $CS_1$  and  $CS_2$  which can be attributed to the buildings

aspect ratio. In  $CS_2$  the slab appears to govern the results as it covers the largest proportion of structure. In  $CS_1$  where larger and more columns were used the influence of the slab in the total cost and carbon is reduced. This suggests that the column grid topology has a significant impact in the optimisation results as it can affect the cost and carbon balance between the slab and the columns.

Similar patterns in the cost and carbon distribution of flat slab structures were also found in previous studies [33,35,57]. The comparison of the results is shown in Table 1. An interesting finding from the analysis of the conventional scenarios is that in both the slab and the columns, the concrete is responsible for almost 2/3 of the total carbon impacts when the steel reinforcement is responsible for only 1/3. This potentially means that thicker slabs and slender columns could result in more efficient carbon structures as small reductions in the carbon of the concrete would reduce the total carbon of the structure. This hypothesis assumes a ratio for the carbon factor of the concrete to the steel between 1/7 and 1/9.

On the other hand, there is a distinct difference in the way cost impacts are distributed between the slab and the columns in the conventional designs. In the columns, the formwork holds the largest proportion of the costs, almost reaching 60% of their total cost. In the slab the situation is more balanced with an equal distribution of the cost between the concrete, reinforcement and formwork costs. These results strongly depend on the cost factors assumed for the formworks: in the columns, the assumption is  $4.52 \text{ £/m}^2$  and  $35.18 \text{ £/m}^2$  for the material and the labour respectively when in the slab is  $5.32 \text{ £/m}^2$  and  $27.58 \text{ £/m}^2$  resulting in almost 17% more expensive cost factor for the columns. This suggests that potential trade-offs between the cost and the carbon performance of the structural elements could occur as the cost computations are not only based on the materials cost but they also include a factor for the associated labour costs.

## 3.3. Optimisation results and discussion

In this section the optimisation results for two building scenarios are presented. In each scenario the solution space is computed based on preferences obtained from the project engineers. Design assumptions, material properties, code requirements and load cases are the same as the actual design scenario. The cost and carbon performance of selected designs were then evaluated against the actual building designs.

### 3.3.1. Algorithmic input

To identify the algorithmic inputs, project engineers were invited to participate in the study via a custom GUI. As the same design assumptions with the actual buildings were used the project



**Table 1**  
Cost and carbon results for the two case studies.

	Total Cost £/m <sup>2</sup>			Total Carbon kgCO <sub>2</sub> e/m <sup>2</sup>		
CS <sub>1</sub>	115.6			135.0		
CS <sub>2</sub>	125.3			153.4		
Contribution of columns in CS <sub>1</sub> total cost	17%			Contribution of columns in CS <sub>1</sub> total carbon		
Contribution of columns in CS <sub>2</sub> total cost	7%			Contribution of columns in CS <sub>2</sub> total carbon		
Contribution of columns in total structure's cost [57]	9%			Contribution of columns in total structure's carbon [57]		
Contribution of columns in total structure's cost [35]	11%					
Contribution of slab in CS <sub>1</sub> total cost	83%			Contribution of slab in CS <sub>1</sub> total carbon		
Contribution of slab in CS <sub>2</sub> total cost	93%			Contribution of slab in CS <sub>2</sub> total carbon		
Contribution of slab in total structure's cost [57]	91%			Contribution of slab in total structure's carbon [57]		
Contribution of slab in total structure's cost [35]	89%					
	Concrete Cost	Reinforcement Cost	Formwork Cost	Concrete Carbon	Reinforcement Carbon	Formwork Carbon
Cost/Carbon Distribution in CS <sub>1</sub> Columns	25%	16%	59%	65%	21%	14%
Cost/Carbon Distribution in CS <sub>2</sub> Columns	22%	14%	64%	64%	19%	17%
Study by [35]	28%	28%	44%	–	–	–
Study by [33]	29%	20%	51%	53%	25%	23%
Cost/Carbon Distribution in CS <sub>1</sub> Slab	32%	33%	35%	68%	29%	3%
Cost/Carbon Distribution in CS <sub>2</sub> Slab	29%	41%	30%	60%	38%	2%
Study by [35]	35%	27%	38%	–	–	–

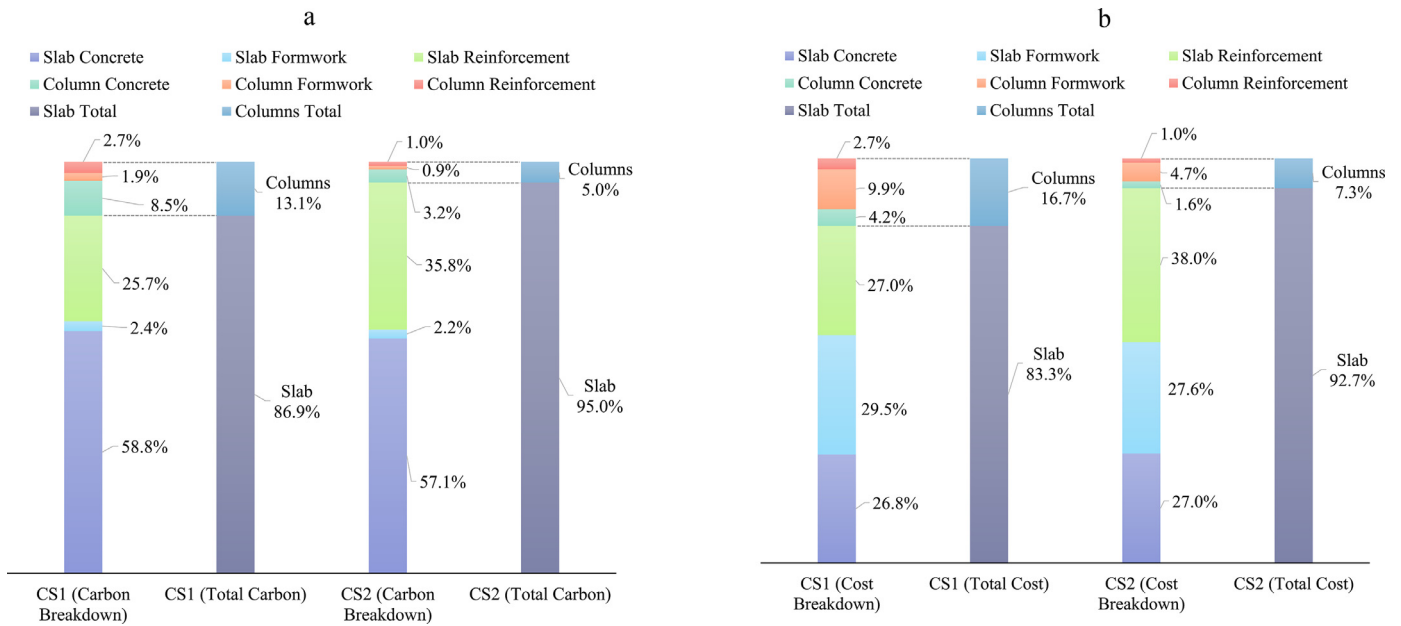


Fig. 6. Carbon (a) and Cost (b) distribution in the case studies.

Table 2  
Input data for NSGA-II algorithm.

Gene	Type	Number of options CS <sub>1</sub>	Design ranges CS <sub>1</sub>	Number of options CS <sub>2</sub>	Design ranges CS <sub>2</sub>	Units
1	Slab thickness	3	225, 250, 275	3	225, 250, 275	mm
2	Column Width	2	225, 250	2	350, 400	mm
3	Column Length	5	800, 850, 900, 950, 1000	3	1200, 1300, 1400	mm
4	Bays X	2*	5, 8	19*	5, 6, 7, 8, 7.5	m
5	Bays Y	8*	5, 6, 7, 7.5, 8, 8.5, 9	19*	5, 6, 7, 8, 7.5	m
6	Bars per column Width	2	2, 3	2	3, 4	Number of bars
7	Bars per column Length	4	4, 5, 6, 8	3	6, 7, 8	Number of bars
Available design combinations		11,520		38,988		

\*As computed from the structural layout algorithm described in Section 2.4.2

engineers were asked to provide design inputs that are the most relevant to each design scenario. If the model is used for the optimisation of speculative or notional building structures where no specific design parameters are classified, then detailed design of experiments would be necessary to recognise the design space for the optimisation process. The seven genes used in this NSGA-II algorithm search and their corresponding ranges correspond to the optimisation levels described in Section 2.4.1 and are summarised in Table 2. Genes 1, 2, 3 are related to sizing parameters of the slab and columns whereas Genes 4, 5 include data for the column grids on X-, Y- directions. Finally, the number of bars needed in the columns is computed using Genes 6, 7. After computing the available grid topologies it is observed that the total number of available design combinations is not the same for the tested scenarios which proves that the optimisation search space in each building will vary depending on the engineers' preferences or other project specific limitations.

The initialisation and genes selection of the optimisation follows a randomised distribution solver. The population size used in the optimisation is 50 and the maximum number of iterations was set to 100. In CS<sub>1</sub> each iteration takes approximately 60 seconds to complete whereas this time is reduced by approximately 35%–40% in CS<sub>2</sub> because of the smaller building size. The computational time also includes the time required to run the FEM model, and obtain detailed material and reinforcement schedules and layouts. Thus, based on the structural outputs from each iteration the algorithmic procedure is considered reasonably efficient as it can significantly reduce the time required for post processing of

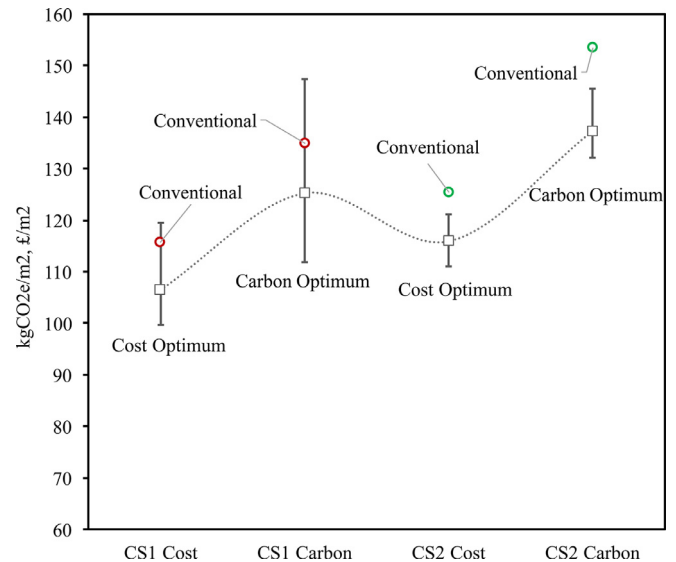


Fig. 7. Optimisation results for the entire CS<sub>1</sub> and CS<sub>2</sub> (CS<sub>1</sub> cost  $\sigma = 5$ , CS<sub>1</sub> carbon  $\sigma = 10.4$ , CS<sub>2</sub> cost  $\sigma = 1.8$ , CS<sub>2</sub> carbon  $\sigma = 2.2$ ).

the optimisation data. Each optimisation simulation performed in this study was computed at least 15 times to provide a consistent solution. A general methodology to identify the number of numerical tests required to provide a statistically robust solution against

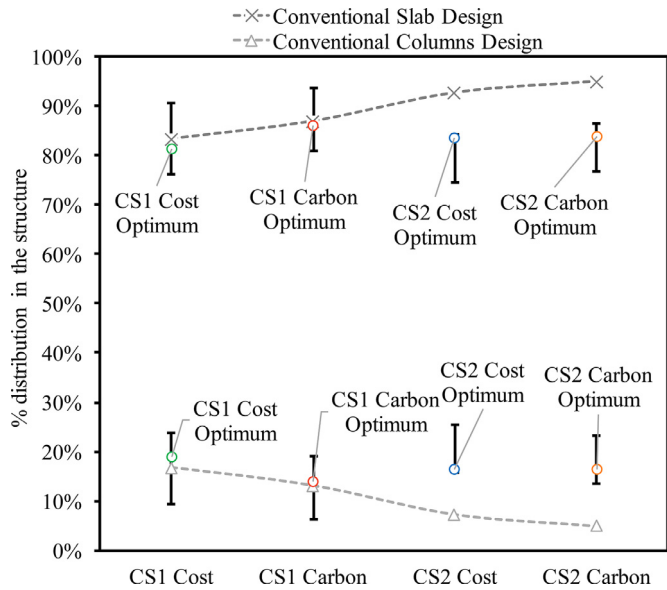


Fig. 8. Cost and carbon distribution in the structure for optimised designs and the conventional designs.

the global optimal solution for a heuristic optimisation problem was proposed by Paya-Zaforteza et al. [58] using the Weibull distribution. A detailed review on statistical optimum estimation techniques for combinatorial optimisation problems can be found in Giddings et al. [59]. However, if necessary the computational time could be further reduced using parallel computing simulations. A sensitivity analysis demonstrated that the computational time is mainly affected by the granularity of the finite element (FE) mesh. In the tested scenarios the mesh consists of 0.5 m sized elements which matches the mesh sizes the project engineers used in their actual analysis. In this way the results could be directly compared. It was also found that denser FE meshes would increase the computational time but could yield more accurate structural calcula-

tions. All computations were performed in a desktop computer using an Intel Core i5-4570 at 3.2 GHz processor with 8GB RAM.

3.3.2. Whole structure analysis

In both building scenarios the entire structural system is optimised using the input data presented in Table 2. The purpose of this analysis is to identify cost and carbon optimum designs and evaluate their performance against the conventional designs. The optimisation routine was repeated at least 15 times to ensure the robustness of the results and the consistency of the convergence. In both scenarios the optimisation algorithm found realistic design alternatives that improve the cost and the carbon performance of the entire structure. In CS<sub>1</sub> the cost and carbon optimum designs are more efficient than the conventional design by 13.7% and 17.1% respectively. On the other hand, the cost and carbon performance of CS<sub>2</sub> could be improved by 11.3% and 13.9% respectively against the conventional design. The results from the optimised cost and carbon functions are plotted in Fig. 7 against the conventional designs. Interestingly enough the distribution of the design space for the two building scenarios vary. Despite the larger available design combinations in CS<sub>2</sub> compared to CS<sub>1</sub>, the optimised solution space appear to be more uniform in terms of cost and carbon results which was also validated by analysing their standard deviations. This can be credited to the smaller structural layout variations (3 uniform configurations in CS<sub>2</sub> compared to 4 variable configurations in CS<sub>1</sub>).

Fig. 8 demonstrates how the cost and the carbon of the structural floors and columns are distributed in the cost and carbon optimum designs. The distributions of the conventional designs are also plotted for reference. It appears that in CS<sub>1</sub> the distribution in the optimum designs closely matches the conventional design whereas in CS<sub>2</sub> large discrepancies are recognised which could suggest that CS<sub>2</sub> is more sensitive to the changes in the slab to columns ratio. In the conventional design of CS<sub>1</sub>, 83% of the structural costs and 87% of the embodied carbon emissions are attributed to the slabs, whereas only 17% of the costs and 13% of the carbon are distributed to the columns. On the other hand, in CS<sub>2</sub> the slabs cost and carbon contributions increase to 93% and 95%

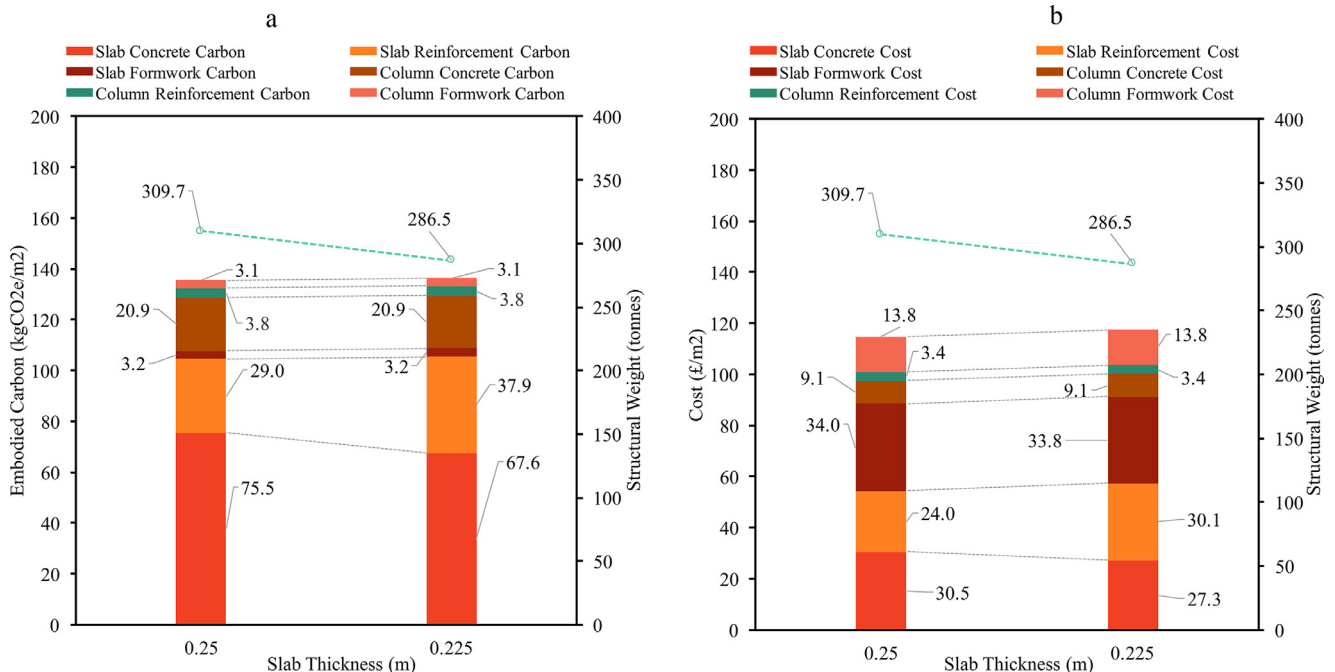
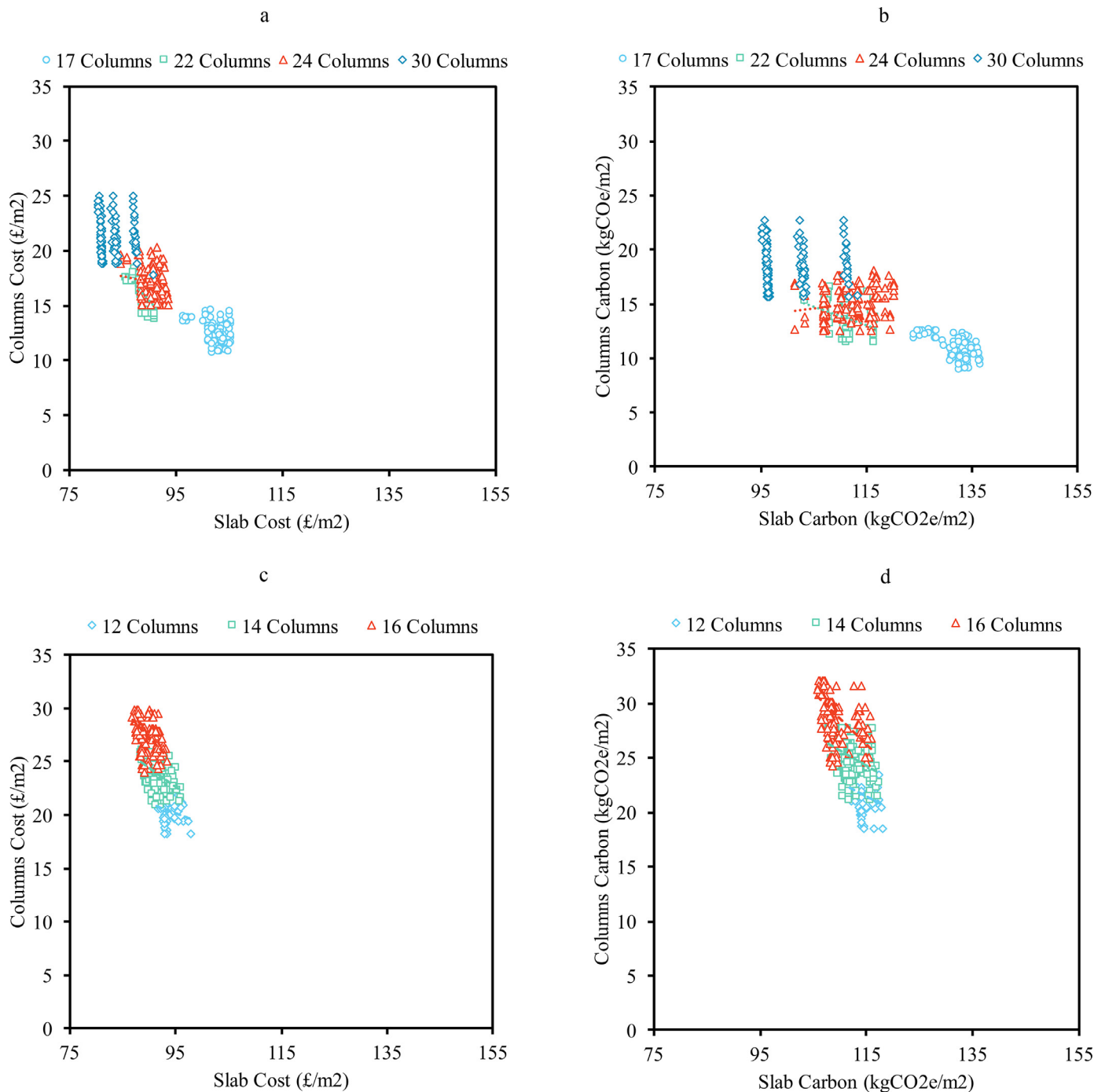


Fig. 9. Relationship between material weight with carbon (a) and cost (b) performance for CS2 considering fixed structural layout, column sizes and reinforcement.



**Fig. 10.** Optimisation analysis between (a) CS<sub>1</sub> slab and columns cost, (b) CS<sub>1</sub> slab and columns carbon, (c) CS<sub>2</sub> slab and columns cost and (d) CS<sub>2</sub> slab and columns carbon.

respectively, whilst the columns cost and carbon distributions decrease to 7% and 5%.

In the cost optimum solution of CS<sub>1</sub>, the distribution between the slabs and columns is 81% and 19% respectively, whereas in the carbon optimum is 86% and 14%. Similar behaviour was observed in the cost and carbon optimum of CS<sub>2</sub> with 84% and 16%. The obtained results can be related to the aspect ratio of the building which consequently affects how the number of columns (structural layout) and slab thickness influence the optimisation results. This is important as in principle it was observed that the optimisation algorithm attempts to find structural solutions with denser

grid layouts and thinner slabs in both buildings as they yield more efficient designs.

Regarding the relationships between the cost and carbon performance of the entire structure a small Pareto front is computed which means that there is only a small trade-off between the cost and carbon solutions for the given design constraints. We found that solutions with minimum carbon and minimum cost vary only by approximately 1–1.5%. Close relationships between the cost and the embodied carbon optimised designs were also reported in previous studies on other structural systems [34,60]. Overall, this behaviour of the cost and the carbon optimum designs, suggests that



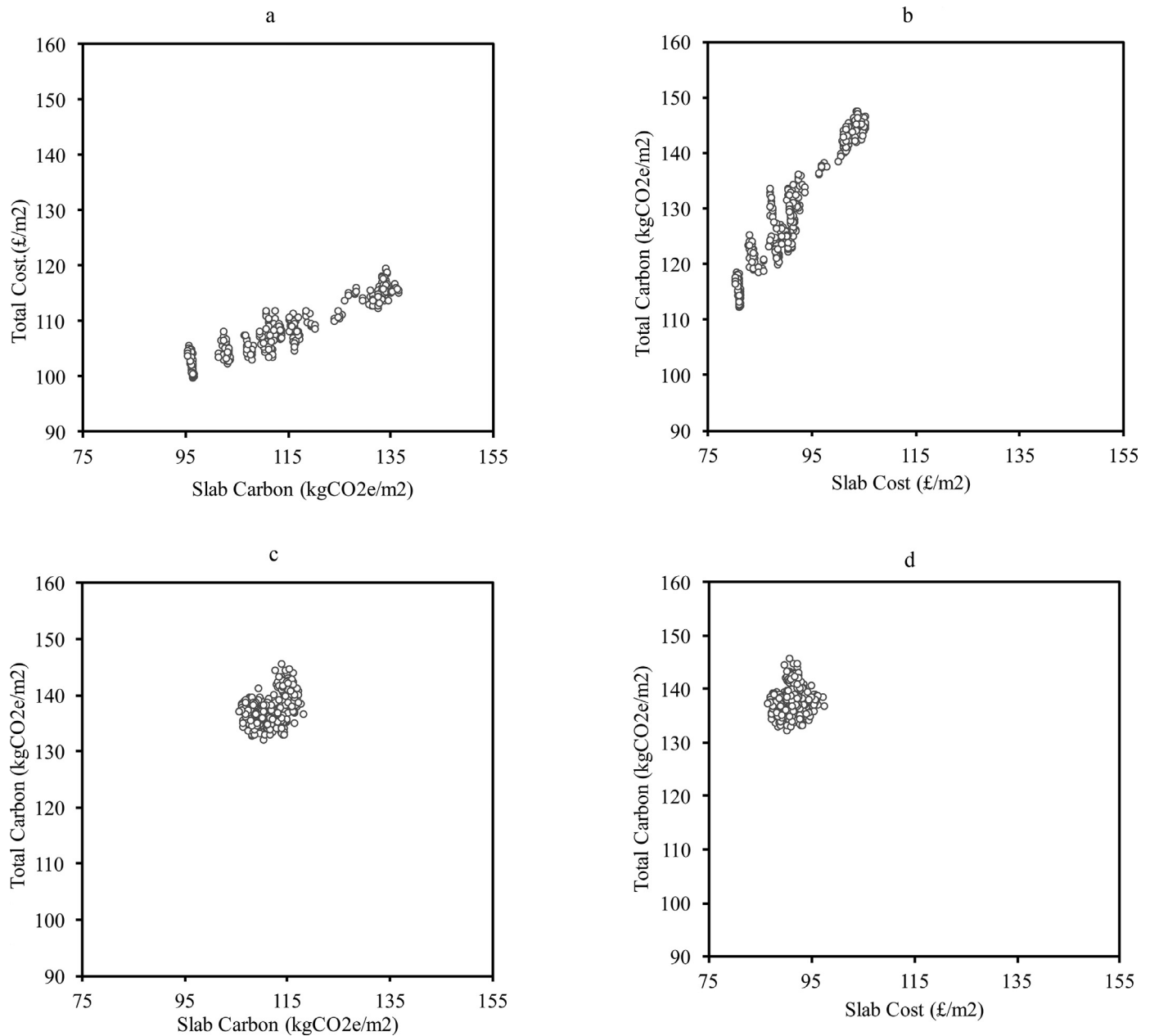


**Fig. 11.** Optimisation analysis between (a) CS<sub>1</sub> total cost with slab carbon, (b) CS<sub>1</sub> total carbon with slab cost, (c) CS<sub>2</sub> total cost with slab carbon and (d) CS<sub>2</sub> total carbon with slab cost.

environmental friendly designs could be obtained with minimal cost increases.

The obtained result depend on the genes granularity and the available input ranges due to the constructability constraints that were applied in the algorithm. In CS<sub>1</sub> both the cost and carbon optimum designs are comparable, comprising 225 mm thick slab and the same 8 × 3 bay configuration (uniform 5 m bays in the X direction and 5 m, 6 m, 5 m bays in the Y direction). However, the columns sizes are different with 800mm×250mm (30 in total) in the cost optimum and 800 mm × 225 mm (30 in total) in the carbon optimum design. On the other hand, in CS<sub>2</sub> the carbon optimum design comprises a 4 × 3 bay configuration with 5 m, 6 m, 5 m, 6 m spans on the X direction and 7 m, 8 m, 7 m spans on the Y direction, 250 mm slab and 1200 mm × 350 mm columns (14 in total). The cost optimum design in CS<sub>2</sub> comprises a 3 × 3 bay configuration with 7.5 m, 7 m, 7.5 m on both X and Y directions and

the same columns (12 in total) and slab sizes with the carbon optimum design. As a general observation, it can be seen that in CS<sub>2</sub> larger variations between the optimum designs occur compared to CS<sub>1</sub>. The building form in CS<sub>2</sub> appears to play a more significant role in the relationship between cost and carbon optimum designs. Besides the obvious differences in the column grids of the optimised designs over the conventional designs the slab thicknesses also appear to vary considerably (250 mm against 225 mm in CS<sub>1</sub> and 250 mm against 275 mm in CS<sub>2</sub>). This is a major design decision that not only influences the structural strategy and the detailing of the floor but it can also influence other decisions associated with the architectural (floor finishes and partitions) or M&E (service integration) strategies.

These results could be partially justified by the close connection between the structural weight and the cost and carbon objective functions. However, solutions with the least total amount

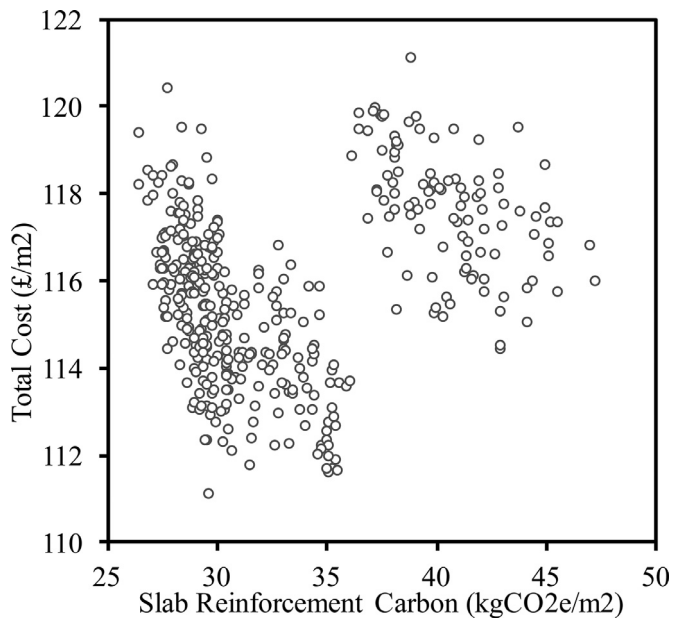


Fig. 12. Optimisation analysis between slab reinforcement carbon and total cost of the structure in CS<sub>2</sub>.

of material are not necessarily the optimum ones in terms of cost or carbon. The ratio between the concrete and the reinforcement weights as well as the structural constraints (e.g. slab deflections) are critical to obtain the optimal solutions. An illustrative example is shown in Fig. 9 for two feasible design options in CS<sub>2</sub>. The structural layout, the column sizes and column reinforcement are fixed whereas two slab options are considered, one with 225 mm slab depth and one with 250 mm. In both options the deflection is less than 30 mm which is the limit provided by the project engineers and thus it is not the governing factor in the optimisation results. One would expect that the option with the 225 mm thick slab would be optimum as it yields the minimum structural weight (286.5 tonnes against 309.7 tonnes). However, Fig. 9 shows that this is not the case for either carbon (Fig. 9a) or cost (Fig. 9b) objectives. The design option with the 250 mm thick slab is more cost and carbon efficient due to the reduced reinforcement in the slab (9 tonnes against 11.8 tonnes). These results are clearly related to the cost and carbon factors used in this study however they provide a good indication about the efficiency of the optimisation procedure and the ability of the penalty functions to guide the search towards optimal solutions. Therefore, more detailed optimisation analyses are performed in the following sections to explore the relationships between the different components of the structure.

### 3.3.3. Structural elements relationships

The functionalities of the multilevel optimisation model are used in this section to understand the detailed cost and carbon relationships between the components of the structure. In practice, this is particularly useful when the entire structural system cannot be fully optimised due to architectural, construction or other project limitations. To perform the relevant computations the objective functions were adjusted accordingly to consider the different structural components.

#### - Structural columns and floors

The cost and carbon functions for the columns and the slabs were used in this optimisation studies. The results from the computations in both buildings and the trade-offs between the structural components are presented in Fig. 10. In CS<sub>1</sub> (Fig. 10a, b) larger trade-offs are observed between the slab and columns cost and

carbon performance when compared with the trade-offs obtained in CS<sub>2</sub> (Fig. 10c, d). These results and trade-off patterns could be associated with the variation of the columns number in the optimised designs. In CS<sub>2</sub> the total number of columns has more uniform distribution of 12, 14 and 16 columns whereas in CS<sub>1</sub> the number of total columns has larger variations (17, 22, 24, 30 columns).

A correlation analysis was conducted (Pearson) and it was found that in both buildings the number of columns has the biggest impact on the cost and carbon results for both the slab and the columns with CS<sub>1</sub>:  $r_{\text{SlabCarbon}} = -0.921$ ,  $r_{\text{SlabCost}} = -0.944$ ,  $r_{\text{ColumnsCarbon}} = 0.869$ ,  $r_{\text{ColumnsCost}} = 0.909$  and CS<sub>2</sub>:  $r_{\text{SlabCarbon}} = -0.710$ ,  $r_{\text{SlabCost}} = -0.715$ ,  $r_{\text{ColumnsCarbon}} = 0.826$ ,  $r_{\text{ColumnsCost}} = 0.880$ . The total number of columns in the structure is calculated directly from Genes 4 and 5. Beside the column grid, in CS<sub>1</sub> the slab thickness is the second more influential parameter in the cost and carbon results of the slabs and the columns. The correlation analysis also demonstrates that in CS<sub>2</sub> the slab thickness is not as significant as in CS<sub>1</sub>. On the other hand, the columns sizes are the most influential parameter in CS<sub>2</sub> after the column grid in both the cost and carbon results for the slab and the columns. These results suggest that the aspect ratio of the building could influence how the cost and carbon is distributed amongst the structural components. A more in depth analysis of the relationships between the slabs and columns with the entire structural system is performed in the subsequent sections.

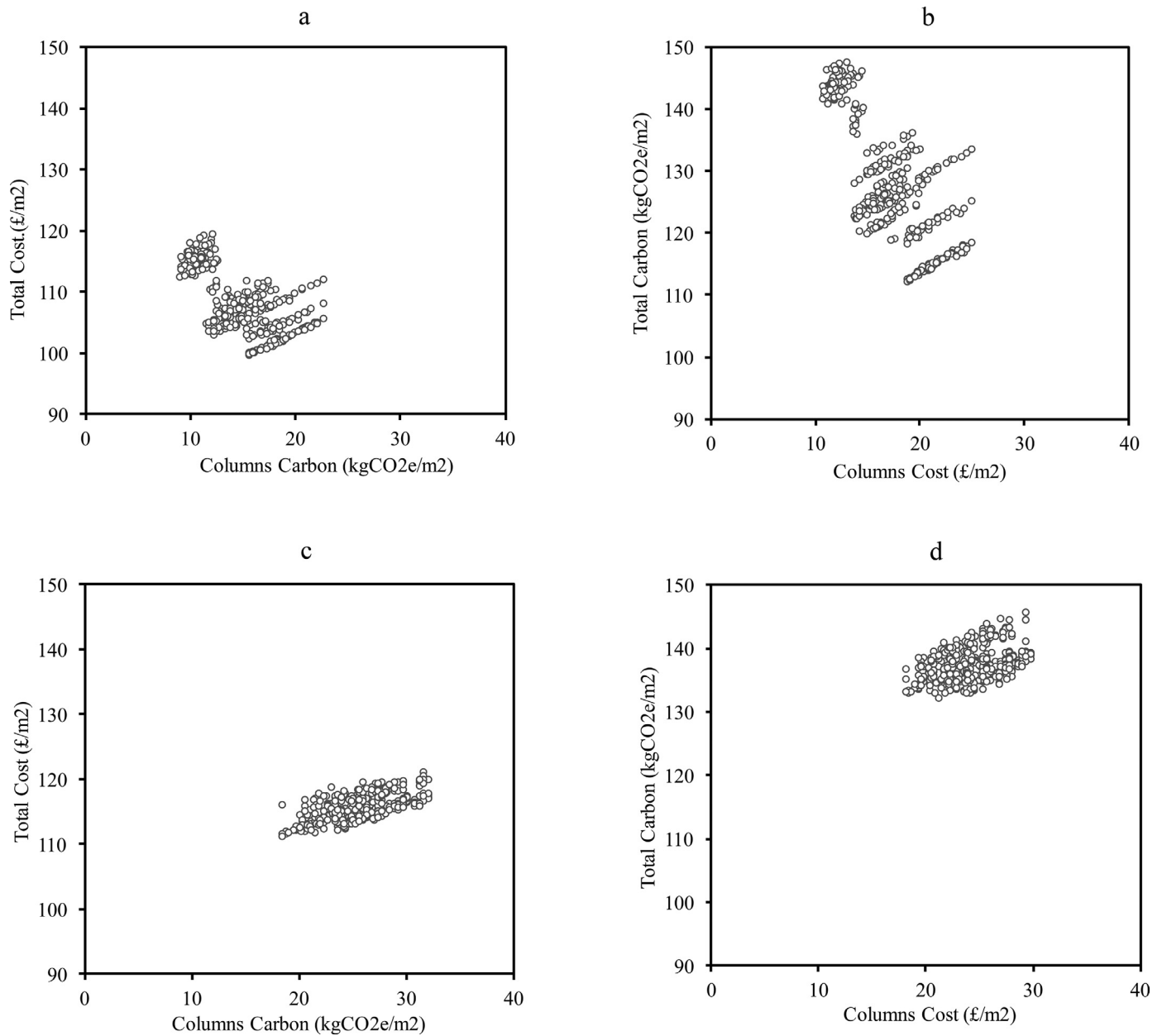
#### - Structural floors and structure

Fig. 11 shows the results from the optimisation iterations for the entire structural system in both buildings and the corresponding slab cost and carbon performance. The results indicate two different optimisation patterns for CS<sub>1</sub> and CS<sub>2</sub>. In CS<sub>1</sub> (Fig. 11a, b) small trade-offs between the structural floor and the entire structure are identified which suggest an almost linear relationship. Similar relationship patterns were identified in the computations of the slab carbon and cost. On the other hand, in CS<sub>2</sub> (Fig. 11c, d) there is a larger Pareto front and a clear trade-off relationship between the cost and carbon performance between the slabs and the entire structure. These findings partially justify the close correlation between the slab thickness and the slab cost and carbon performance which was described in the previous section.

More detailed interactions between the slab components and the whole structure could also be computed by the multilevel optimisation procedure yielding more informed design assessments. The granularity of the optimisation analysis is easily adjusted by the structural engineers by specifying more refined sampling optimisation parameters. A descriptive example is shown in Figure 12 which visualises the optimisation results and the obtained trade-offs between the entire structure with the slab reinforcement for CS<sub>2</sub>. Similar relationships with the concrete or the formwork components of the slab could be computed by adjusting the objective functions' modules. Overall, the results show that the optimisation model can effectively classify the different requirements between the two building typologies and compute their relationships.

#### - Structural columns and structure

In this section the relationships between the structural columns and the entire structure are investigated. Fig. 13 shows the results obtained from the optimisation analysis in this simulation set. Fig. 13a, b presents the trade-off relationships between the total cost and carbon and the cost and carbon performance of the columns. In CS<sub>2</sub> on the other hand, an almost linear relationship between the structural columns and the entire structure was identified (Fig. 13c, d).



**Fig. 13.** Optimisation analysis between (a) CS<sub>1</sub> total cost with columns carbon, (b) CS<sub>1</sub> total carbon with columns cost, (c) CS<sub>2</sub> total cost with columns carbon and (d) CS<sub>2</sub> total carbon with columns cost.

Comparing the results from Figs. 11 and 13 it becomes apparent that there are significant differences in the optimisation patterns and the relationships between the structural columns and floors for the two buildings. These findings are associated to the general building form and particularly with the ratio of structural columns over the total slab area. Overall, detailed optimisation analysis using the proposed multilevel procedure could provide new insights and a better understanding on how these relationships are developed in each building typology. Further analysis on the impact of building form in the optimisation of the RC structure is recommended. For instance, U- or L-shaped buildings or other core locations could also be investigated to establish a more comprehensive specification of these relationships.

## 4. Summary and recommendations

### 4.1. Building level implications

The optimisation approach presented in the previous sections could be used by engineers and other decision makers such as architects or clients for early design decisions. The utilisation of BIM data offers numerous opportunities for integration with other building system analysis and decision-making modules [40]. The main intention of the analysis at this level is to prompt discussions around the cost and carbon efficiency of the structural systems and evaluate the feasibility of design alternatives populated by the optimisation model. The analysis highlighted the design parameters of the structure that drive the cost and carbon performance. Overall, it was found that the column layout and the form

of the building play a significant role in the overall cost and carbon performance of the structure and the balance between the cost and carbon performance of the constituent structural components. At building level, these findings are significant as they suggest that the final design decisions would need to be effectively coordinated with the broader design team. This is because alterations in the internal layout of the building or in the entire building form cannot be decided only by the structural engineers.

#### 4.2. Contextual considerations

It is evident that comparing the conventional design with the optimised solutions is not easy and can only provide a retrospective assessment as the building is already under construction and no further changes could be suggested by the design team. However, the proposed optimisation approach can be particularly useful during the early phases of the design development when basic information about the building's massing and boundaries become available. Early BIM models could be used to provide design guidance to structural engineers using criteria relevant to each project. In addition, the optimised solutions could be used as potential cost and carbon performance benchmarks for a given structure. Any future design iterations of the structural system explored by the engineers will be compared against those optimisation benchmarks as the required cost and carbon performance for the different designs is embedded in the BIM model. By doing so more informed decisions could be expected when the cost and carbon implications of the different design alternatives are effectively quantified. Currently when a project begins such information is rarely available which often leads to vagueness around the capabilities of the proposed design configurations. It is expected that similar benchmark strategies of building structures will become widely available in the future with the expansion of BIM capabilities in the construction industry and the possible establishment of structural efficiency limits in the national codes.

#### 4.3. Conclusions

As building design and construction practices move into the era of big data, rich information technologies and integrated project delivery, the traditional structural optimisation procedures would have to be adjusted accordingly. BIM technologies offer the computational platforms to achieve this transition. The study explored a body of research which has received limited consideration in the past and involves the integration of heuristic optimisation procedures within BIM technologies. The proposed computational workflow comprised a BIM-integrated multi-objective optimisation approach for reinforced concrete structures which is supported by FEM utilising cost and carbon objective functions. The multilevel optimisation model takes place in three main levels comprising column layouts, members sizing and reinforcement detailing. Rigorous testing of the corresponding computational modules with the integrated constructability constraints was presented in the paper. The optimisation approach was validated using actual building scenarios. Results demonstrated that the optimisation methodology can effectively compute solutions that improve the cost and carbon performance of the conventional designs without compromising their constructability. The topology of the structural grid appeared to have the largest impact on the cost and carbon performance of the structure and thus the implications in the architectural layouts of the building need to be further investigated. It was also observed that small trade-offs occur between the cost and carbon optimum designs for the entire structure which suggests that carbon optimum designs could be obtained with minimal cost increases. Finally, it was found that the distribution of cost and carbon

between the different elements in the structure vary depending on the building form.

#### Acknowledgements

This research has been made possible through funding provided by the Engineering and Physical Sciences Research Council (EPSRC) and from Price & Myers LLP via the UCL EngD Centre (Grant number: EP/G037159/1) in Virtual Environments, Interaction and Visualisation and this is gratefully acknowledged here.

#### References

- [1] A. Adamu, B. Karihaloo, G. Rozvany, Minimum cost design of reinforced concrete beams using continuum-type optimality criteria, *Struct. Optim.* 7 (1994) 91–102.
- [2] C. Camp, A. Assadollahi, CO2 and cost optimization of reinforced concrete footings using a hybrid big bang-big crunch algorithm, *Struct. Multidiscip. Optim.* 48 (2013) 411–426.
- [3] B. Gencturk, Life-cycle cost assessment of RC and ECC frames using structural Optimization, *Earthquake Eng. Struct. Dyn.* 42 (2013) 61–79.
- [4] M. Khajehzadeh, M. Taha, M. Eslami, Multi-objective optimisation of retaining walls using hybrid adaptive gravitational search algorithm, *Civil Eng. Environ. Syst.* 31 (3) (2014) 229–242.
- [5] F. Martinez-Martin, F. Gonzalez-Vidosa, A. Hospitaler, V. Yepes, Multi-objective optimization design of bridge piers with hybrid heuristic algorithms, *J. Zhejiang Univ.-Sci. A* 13 (6) (2012) 420–432.
- [6] T. Garcia-Segura, V. Yepes, J. Marti, J. Alcalá, Optimization of concrete I-beams using a new hybrid glowworm swarm algorithm, *Latin Am. J. Solids Struct.* 11 (7) (2014) 1190–1205.
- [7] D. Miller, J.-H. Doh, Incorporating sustainable development principles into building design: a review from a structural perspective including case study, *Struct. Des. Tall Spec. Build.* 24 (6) (2014) 421–439.
- [8] W. Chong, S. Kumar, C. Haas, S. Beheiry, L. Coplen, M. Oey, Understanding and interpreting baseline perceptions of sustainability in construction among civil engineers in the United States, *J. Manag. Eng.* 25 (July (3)) (2009) 143–154.
- [9] V. Yepes, F. Gonzalez-Vidosa, J. Alcalá, P. Villalba, CO2-optimization design of reinforced concrete retaining walls based on a VNS-threshold acceptance strategy, *J. Comput. Civil Eng.* 26 (3) (2012) 378–386.
- [10] N. Blismas, C. Pasquire, A. Gibb, Benefit evaluation for off-site production in construction, *Construct. Manag. Econ.* 24 (2) (2006) 121–130.
- [11] I. Paya-Zaforteza, V. Yepes, A. Hospitaler, F. González-Vidosa, CO2-optimization of reinforced concrete frames by simulated annealing, *Eng. Struct.* 31 (2009) 1501–1508.
- [12] W. Wang, R. Zmeureanu, H. Rivard, Applying multi-objective genetic algorithms in green building design optimization, *Build. Environ.* 40 (2005) 1512–1525.
- [13] Y. Pei, Y. Xia, Design of reinforced cantilever retaining walls using heuristic optimization algorithms, *Proc. Earth Planet. Sci.* 5 (2012) 32–36.
- [14] C. Perea, J. Alcalá, V. Yepes, F. Gonzalez-Vidosa, A. Hospitaler, Design of reinforced concrete bridge frames by heuristic optimization, *Adv. Eng. Softw.* 39 (2008) 676–688.
- [15] A. Carbonell, F. Gonzalez-Vidosa, V. Yepes, Design of reinforced concrete road vaults by heuristic optimization, *Adv. Eng. Softw.* 42 (2011) 151–159.
- [16] C. Camp, A. Akin, Design of retaining walls using big bang- crunch optimization, *J. Struct. Eng.* 138 (3) (2012) 438–448.
- [17] S. Babiker, F. Adam, A. Mohamed, Design optimization of reinforced concrete beams using artificial neural network, *Int. J. Eng. Invent.* 1 (8) (2012) 07–13.
- [18] A. Aga, F. Adam, Design optimization of reinforced concrete frames, *Open J. Civil Eng.* 5 (2015) 74–83.
- [19] M. Ismail, "Design optimization of structural concrete beams using genetic algorithms," 2007.
- [20] M. Khajehzadeh, M. Taha, A. El-Shafie, M. Eslami, Modified particle swarm optimization for optimum design of spread footing and retaining wall, *J. Zhejiang Univ.-Sci. A* 12 (6) (2011) 415–427.
- [21] M. Ghazavi, S. Bonab, Optimization Of Reinforced Concrete Retaining Walls Using Ant Colony Method, 2011 Munich, Germany.
- [22] R. Rao, A material selection model using graph theory and matrix approach, *Mater. Sci. Eng. A* 431 (2006) 248–255.
- [23] S. Lu, I. Wu, B. Hsiung, Applying building information modelling in environmental impact assessment for urban deep excavation projects, *Gerontechnology* 11 (2) (2009).
- [24] V. Selvi, R. Umarani, Comparative analysis of ant colony and particle swarm optimization techniques, *Int. J. Comput. Appl.* 5 (4) (2010) 1–6.
- [25] H. Yapa, J. Lees, Optimisation of shear strengthened reinforced concrete beams, *Eng. Comput. Mech.* 167 (June (EM2)) (2014) 82–96.
- [26] G. Zavala, A. Nebro, F. Luna, C. Coello Coello, A survey of multi-objective meta-heuristics applied to structural optimization, *Struct. Multidiscip. Optim.* 49 (April (4)) (2014) 537–558.
- [27] J. Marti, V. Yepes, F. Gonzalez-Vidosa, Memetic algorithm approach to designing precast-prestressed concrete road bridges with steel fiber reinforcement, *J. Struct. Eng.* 141 (2) (2015) 04014114-1 - 04014114-9.



- [28] I. Boussaid, J. Lepagnot, P. Siarry, A survey on optimization metaheuristics, *Inf. Sci.* 237 (2013) 82–117.
- [29] A. Kosloski, "Cost and Embodied Energy Optimisation of rectangular reinforced concrete beams," Clemson University, All Theses, Paper 1776, Clemson University, 2014.
- [30] D. Yeo, R. Gabbai, Sustainable design of reinforced concrete structures through embodied energy optimization, *Energy Build.* 43 (2011) 2028–2033.
- [31] C. Camp, F. Huq, CO<sub>2</sub> and cost optimization of reinforced concrete frames using a big bang-big crunch algorithm, *Eng. Struct.* 48 (2013) 363–372.
- [32] D. Yeo, F. Potra, Sustainable design of reinforced concrete structures through CO<sub>2</sub> emission optimisation, *J. Struct. Eng.* 141 (2015) Special Issue: Sustainable Building Structures, B4014002.
- [33] F. Medeiros, M. Kripka, Optimization of reinforced concrete columns according to different environmental impact assessment parameters, *Eng. Struct.* 59 (2014) 185–194.
- [34] H. Park, H. Lee, Y. Kim, T. Hong, S. Choi, Evaluation of the influence of design factors on the CO<sub>2</sub> emissions and costs of reinforced concrete columns, *Energy Build.* 82 (2014) 378–384.
- [35] M. Sahab, A. Ashour, V. Toropov, Cost optimisation of reinforced concrete flat slab buildings, *Eng. Struct.* 27 (2005) 313–322.
- [36] P. Sharafi, M. Hadi, L. Teh, Heuristic Approach for optimum cost and layout design of 3D reinforced concrete frames, *J. Struct. Eng.* 138 (2012) 853–863.
- [37] M. Aldwaik, H. Adeli, Cost optimization of reinforced concrete flat slabs of arbitrary configuration in irregular highrise building structures, *Struct. Multidisc. Optim.* 54 (2016) 151–164.
- [38] P. Foraboschi, M. Mercanzin, D. Trabucco, Sustainable structural design of tall buildings based on embodied energy, *Energy Build.* 68 (2014) 254–269.
- [39] J. Fernandez-Ceniceros, R. Fernandez-Martinez, E. Fraile-Garcia, F. Martinez-de-Pison, Decision support model for one-way floor slab design: A sustainable approach, *Autom. Constr.* 35 (2013) 460–470.
- [40] S. Eleftheriadis, D. Mumovic, P. Greening, Life cycle energy efficiency in building structures: a review of current developments and future outlooks based on BIM capabilities, *Renew. Sustain. Energy Rev.* 67 (2017) 811–825.
- [41] S. Eleftheriadis, D. Mumovic, P. Greening, A. Chronis, BIM enabled optimisation framework for environmentally responsible and structurally efficient design systems, in: *Proceedings of the 32nd International Symposium on Automation and Robotics in Construction and Mining: Connected to the Future*, Oulu, Finland, 2015.
- [42] A. Smith, D. Coit, Constraint-handling techniques - penalty functions, *Handbook of Evolutionary Computation*, Institute of Physics Publishing and Oxford, University Press, Bristol, U.K., 1997 p. Chapter C5.2.
- [43] A. Fisher, S. Sharma, 2010. [Online]. Available: [Accessed 20 06 2017] [http://bimandbeam.typepad.com/AUTODESKROBOT\\_structuralanalysisprofessional\\_WHITEPAPER\\_final.pdf](http://bimandbeam.typepad.com/AUTODESKROBOT_structuralanalysisprofessional_WHITEPAPER_final.pdf).
- [44] K. Deb, A. Pratap, S. Agarwal, T. Meyarivan, A fast and elitist multiobjective genetic algorithm: NSGA-II, *IEEE Trans. Evolution. Comput.* 6 (2) (2002) 182–197.
- [45] T. Vo-Duy, D. Duong-Gia, V. HO-Huu, H. Vu-Do, T. Nguyen-Thoi, Multi-objective optimization of laminated composite beam structures using NSGA-II algorithm, *Compos. Struct.* 168 (2017) 498–509.
- [46] C. De Wolf, *Low Carbon Pathways to Structural Design: Embodied Life Cycle Impacts of Building Structures*, Massachusetts Institute of Technology, Cambridge, MA, 2017.
- [47] F. Pomponi, A. Moncaster, Scrutinising embodied carbon in buildings: the next performance gap made manifest, *Renew. Sustain. Energy Rev.* (2017).
- [48] C. Chau, T. Leung, W. Ng, A review on life cycle assessment, life cycle energy assessment and life cycle carbon emissions assessment on buildings, *Appl. Energy* 143 (2015) 395–413.
- [49] M. Webster, H. Meryman, A. Slivers, T. Rodriguez-Nikl, L. Lemay, K. Simonen, *Structure and Carbon - How Materials Affect the Climate*, American Society of Civil Engineers (ASCE), Reston, VA, 2012.
- [50] J. Gregory, A. Noshadravan, E. Olivetti, R. Kirchain, A methodology for robust comparative life cycle assessments incorporating uncertainty, *Environ. Sci. Technol.* 50 (12) (2016) 6397–6405.
- [51] AECOM, *Spon's Architect's and Builders' Price Book 2017*, Taylor and Francis, 2016.
- [52] S. Coons, *Surfaces For Computer-Aided Design of Space Forms*, Massachusetts Institute of Technology, Cambridge, MA, USA, 1967.
- [53] R.H. Wood, The reinforcement of slabs in accordance with a predetermined field of moments, *Concrete* 2 (2) (1968) 69–76.
- [54] R. Wood, G. ARmer, A. Hillerborg, The theory of the strip method for design of slabs, *Proc. Inst. Civ. Eng.* 41 (2) (1968) 285–311.
- [55] SteelConstruction.info, "Whole life embodied CO<sub>2</sub> emissions data," [Online]. Available: [http://www.steelconstruction.info/Life\\_cycle\\_assessment\\_and\\_embodied\\_carbon](http://www.steelconstruction.info/Life_cycle_assessment_and_embodied_carbon). [Accessed 04 July 2017].
- [56] WoodforGood, "Plywood Assuming 100% recycling at the end of life stage," [Online]. Available: <https://woodforgood.com/lifecycle-database/structural-products/>. [Accessed 04 July 2017].
- [57] S. Eleftheriadis, P. Duffour, P. Greening, J. James, D. Mumovic, Multilevel computational model for cost and carbon optimisation of reinforced concrete floor systems, *34th International Symposium on Automation and Robotics in Construction (ISARC 2017)*, 2017.
- [58] I. Paya-Zaforteza, V. Yepes, F. Gonzalez-Vidosa, A. Hospitaler, On the Weibull cost estimation of building frames designed by simulated annealing, *Meccanica* 45 (2010) 693–704.
- [59] A. Giddings, R. Rardin, R. Uzsoy, Statistical optimum estimation techniques for combinatorial optimization problems: a review and critique, *J. Heuristics* 20 (2014) 329–358.
- [60] H. Park, B. Kwon, Y. Shin, Y. Kim, T. Hong, S. Choi, Cost and CO<sub>2</sub> emission optimization of steel reinforced concrete columns in high-rise buildings, *Energies* 6 (11) (2013) 5609–5624.